Aerodynamic Force Characterization of a Novel Variable Amplitude Flapping Wing Robot

Geourg Kivijian* and Nandeesh Hiremath†
Department of Aerospace Engineering, California Polytechnic State University, San Luis Obispo, CA, 93405

Flapping-wing aerial vehicles (FWAVs) have long been inspired by the efficiency and maneuverability of bird flight. However, most existing FWAVs rely on fixed-amplitude geared flapping mechanisms, limiting their ability to adapt across flight regimes such as takeoff, cruising, and landing. To address this limitation, a novel Field-Oriented Control (FOC) cable-driven variable amplitude flapping mechanism has been developed, enabling dynamic control over both flapping frequency and amplitude. This study presents the first experimental evaluation of the aerodynamic forces generated by this biomimetic system at varying flapping amplitudes.

To quantify the aerodynamic performance of the flapping mechanism, a six-degree-of-freedom (6DOF) load cell measurement is taken capable of measuring cycle-averaged lift and thrust forces. A range of flapping amplitudes is tested to assess how these parameters influence force production. The collected force data are processed to generate time-averaged lift and thrust plots as a function of stroke amplitude, providing critical insight into optimal operating conditions for flight.

The results are compared with theoretical modeling for ideal amplitude in FWAV design and this study will inform future work flight testing the FWAV named K1 that utilizes the novel drive mechanism. The proposed and tested flapping methodology here aims to provide a robust framework for future ornithopter flapping mechanisms, pushing the field closer to achieving fully articulated, multi-modal flight akin to biological birds.

I. Nomenclature

FWAV	=	Flapping Wing Aerial Vehicle
VAF	=	Variable Amplitude Flapping
RPM	=	Revolutions Per Minute
FOC	=	Field Oriented Control
UAV	=	Unmanned Aerial Vehicles
RC	=	Remote Control
PWM	=	Pulse Width Modulation
UART	=	Universal Asynchronous Receiver-Transmitter Communication Protocol
COTS	=	Commercial-Off-The-Shelf
ADC	=	Analog to Digital Converter

II. Introduction

Flapping Wing Aerial Vehicles are continuously being studied and refined with higher fidelity simulations and physical models. With the ideal performance of an FWAV being to match the characteristic efficiency, control, and overall capability of avian flight, increased focus on bio-mimetics and implementation of more refined design is gaining traction in research labs pursuing FWAVs.

Most of these advancements in recent of FWAV and bird-inspired UAS systems optimize the wing and tails, but the flapping amplitude is often overlooked[1–4]. This is due to most designs being optimized to fly at steady-level flight conditions where flapping amplitude stays relatively constant and flapping frequency is the sole active parameter.

*Graduate Researcher, Department of Aerospace Engineering, California Polytechnic State University, San Luis Obispo, CA, 93405, AIAA Member: 1400184

†Assistant Professor, Department of Aerospace Engineering, California Polytechnic State University, San Luis Obispo, CA, 93405, AIAA Member: 1372347

Birds on the other hand use variable amplitude flapping (VAF) while taking off, descending, and conducting many acrobatic maneuvers[5–7]. Without VAF it is impossible to achieve the full articulation and flight capabilities that we see in avian flight.

The most common flapping mechanism design is the fixed-gear, fixed-linkage setup that varies frequency using motor RPM but has a fixed amplitude due to the linkages and gear size being fixed in operation. To generate VAF existing designs have attempted solutions [8–10]. The issue is that these current designs lack efficiency, power density, or are too complex and heavy for the reliable operation needs of FWAVs.

In this paper, we explore the lift and thrust generated by K1 , an ornithopter that utilizes a novel bio-mimetic variable-amplitude flapping mechanism that is driven by a brushless motor controlled by an FOC drive board. The flapping mechanism, test setup, and the results of variable amplitude testing (between 10°-90°) will all be discussed here.

III. Flapping Mechanism and K1 FWAV

The novel flapping mechanism uses field oriented control to control a brushless motor to oscillate at high frequencies back and forth. Please refer to figures 1 and 2 below to understand the mechanism. The system uses an ODrive S1 unit and a modified 460kv 3506 brushless motor mounted together. The motor mount, including the rest of the structure is a hybrid 3D-printed and pultruded carbon tube structure to be stiff, yet easily workable, and lightweight.

The motor drives the flapping motion of the wings utilizing a biomimetic push-pull cable drive mechanism that also serves as the main gear reduction of the system. As seen in Figure 1, the design replicates the function of avian pectoralis and supracoracoideus muscles by pulling on downstroke and upstroke respectively with motor oscillation. To handle the high aerodynamic and inertial torques that will be experienced by the wing, the cables are UHMWPE rope preloaded and tensioned for zero slack.

The ODrive is fed a control signal via an onboard Teensy 4.0 microcontroller to generate the sinusoidal motion necessary for flight and in this case testing. Communication between the user and Teensy is PWM through an RC Transmitter, and the Teensy pushes positional commands through UART to the ODrive. Any oscillatory signal is capable of being generated as long as it is continuous and it does not exceed the physical bounds of the system. Overall the system is capable of operating at a maximum of 8 Hz at 180 degrees of peak-peak flapping amplitude covering most avian species capabilities.

K1 is the FWAV that houses the novel drive mechanism as described and is used for testing the system. K1 has a wingspan of 1 meter and an overall wing surface area of 0.175 square-meters. The wings are made of 40D Ripstop nylon, sparred with carbon fiber rods in various orientations and thicknesses in order to produce an ideal amount of torsional planar bending for thrust generation.

An image of K1 assembled can be seen in Figure 2. The horizontal and vertical stabilizers (tail) on K1 were removed as it was deemed unnecessary for the loading tests.

IV. Experimental Setup and Methodology

The experimental setup for testing the lift and thrust forces generated by K1 at varying amplitudes is as follows:

A. 6DOF Load Cell

The load cell as pictured in Figure 2 is the customizable 6DOF load cell developed by fellow Cal Poly Aerospace Graduate Student Pyeongkang Kim [11]. It features 6 COTS bar style load cells, paired with 6 EMBSGB200M amplifiers. Wired to a National Instruments NI USB-6218 DAQ, the onboard 16 bit ADC gives a resolution of 0.1525 grams which is more than enough for our needs. The amplifier cutoff frequency is at 65 Hz.

The load cell is mounted onto two 1.5"x3" 80-20 Aluminum Extrusion bars which are clamped to the table. Two iron blocks are also placed to dampen and increase the stability of the test setup. From the center of the Load Cell, a 12 mm Carbon Fiber Rod is mounted vertically towards an attachment point under K1. The Carbon Fiber rod extends 0.5 m from the load cell platform to reduce the aerodynamic effect of obstructions to the wing flapping wakes. The load cells are tuned for higher sensitivities in the Lift and Thrust directions. For the current studies, only wind-off cases are shown to verify the response of the frequency and amplitude of flapping with the periodic lift and cycle averaged lift.

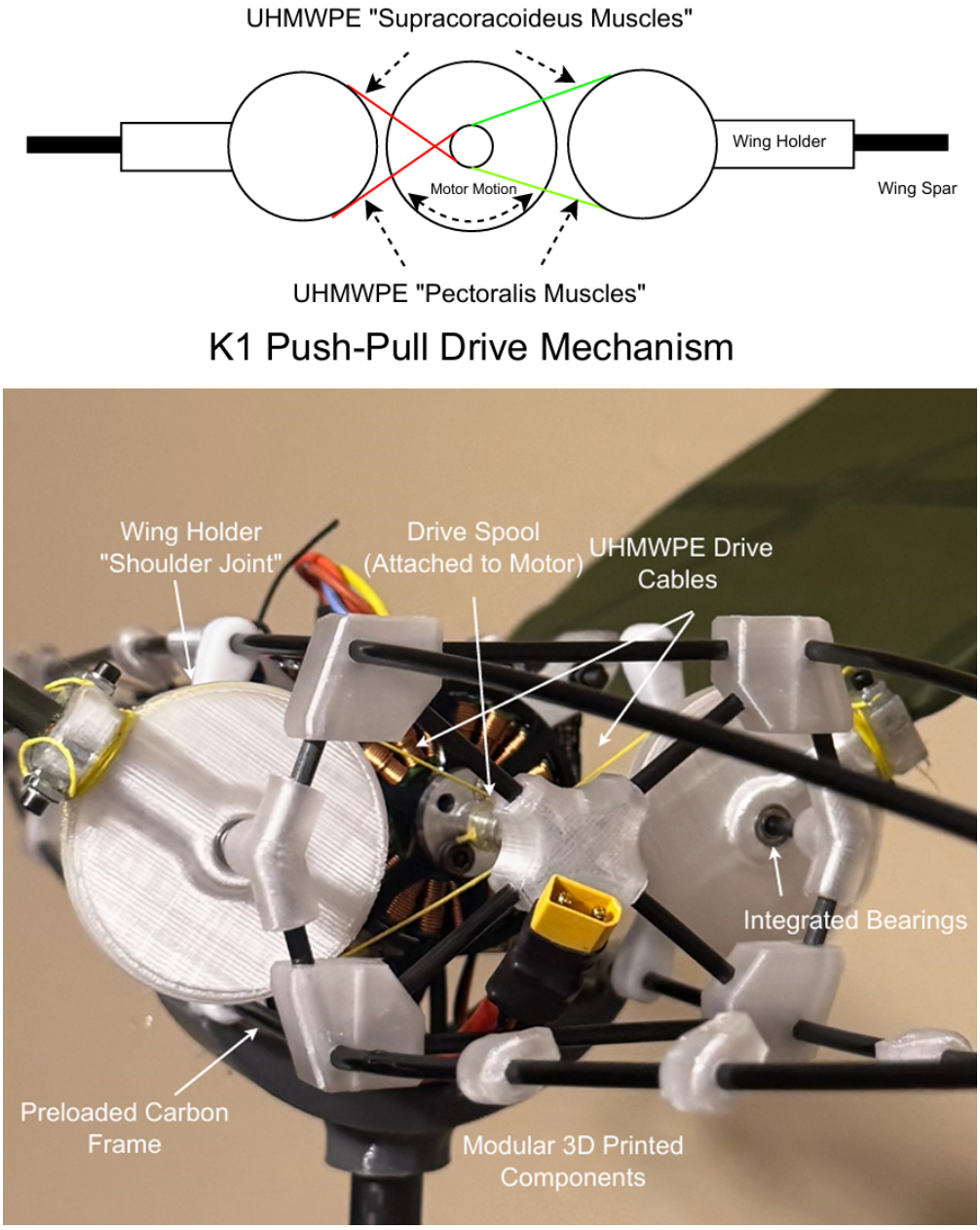

Fig. 1 Flapping Mechanism Diagram and K1 Flapping Mechanism

B. K1 Test Setup

The test setup implemented on K1 is adjusted in 2 ways. Initially, the wing used has a semi-span (root-tip) of 0.5 m, and a projected area of 0.0875 square meters totaling 0.175 square meters of wing surface area to be tested. The wings are press-fit into the respective wing joints and allowed to rotate freely. There is a net dihedral set of 7° and the following amplitude sweep (flapping angle) measurements use this angle as the datum.

Second, K1's onboard Teensy flight computer is loaded with code to generate a test sine wave. This testing code sets the signal to a fixed frequency of 4 Hz and varies the amplitude by increasing the flapping angle by 10 degrees every 5 seconds. The starting peak-peak amplitude is set at 10 degrees and sweeps to a final peak-peak amplitude of 90 degrees over 9 intervals.

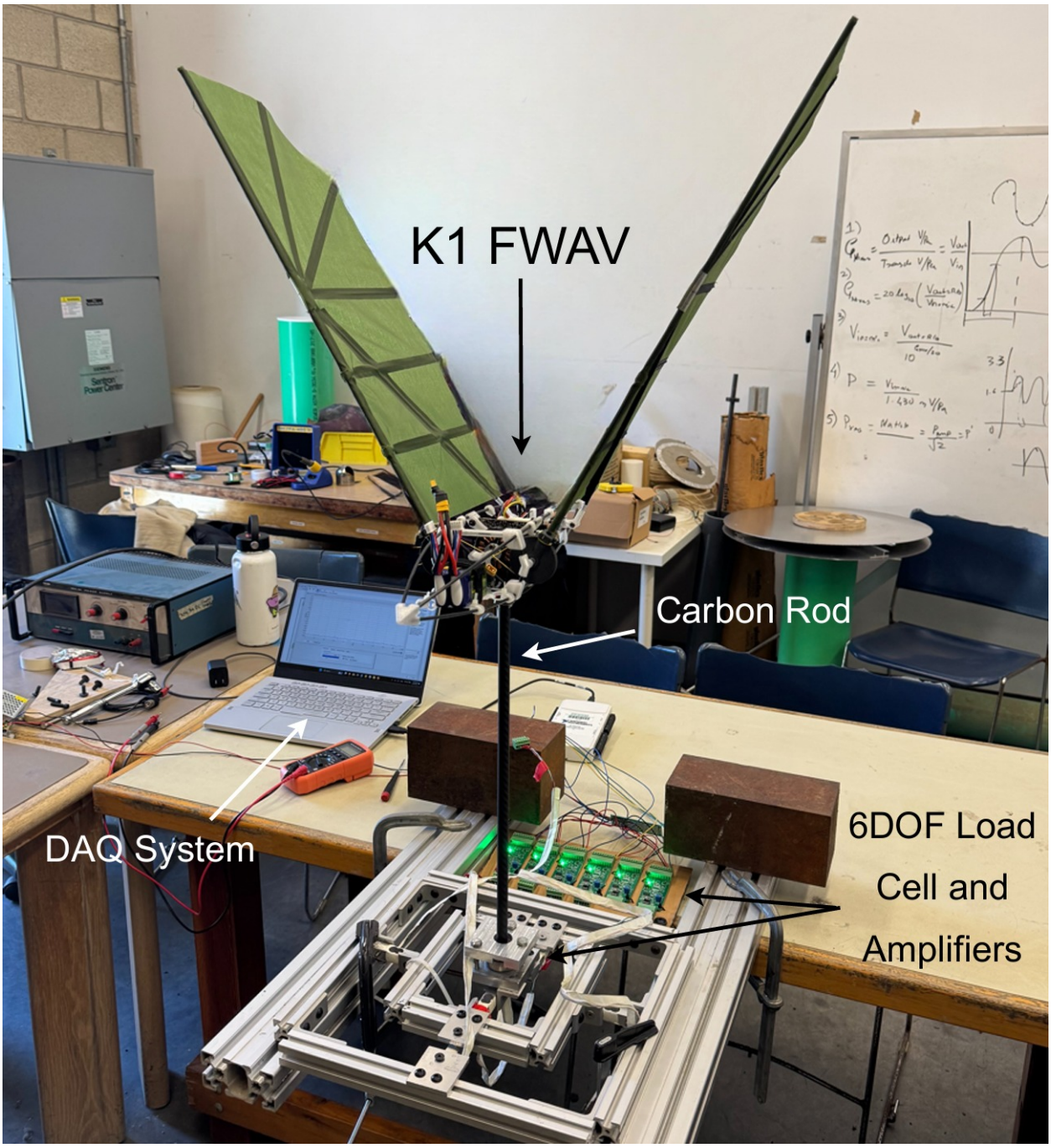

Fig. 2 Test Setup of K1 Mounted on 6-DOF Load Cell

C. Methodology

K1 is powered on and the dihedral angle is set. The load cells are then tared by the operator and data recording begins. K1 is then commanded to begin the testing sequence, which sweeps through the full set of amplitudes commanded. Concurrently, a video recorder captures the motion of K1 allowing for validation of the commanded angles as seen in Figure 3. Following the testing, data analysis was conducted on MATLAB where the time varying loads were analyzed.

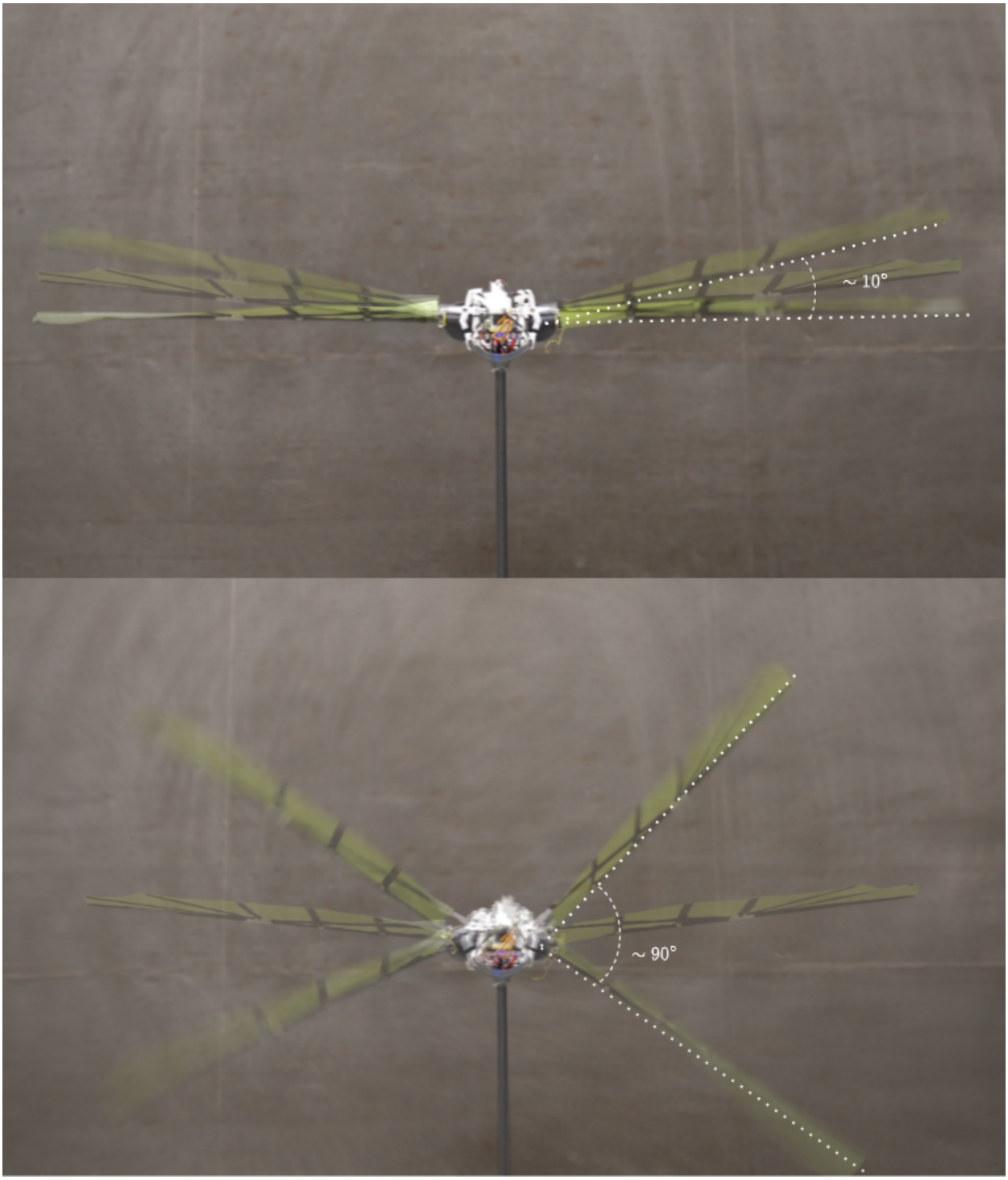

Fig. 3 Minimum and Maximum Flapping Angles Tested

V. Results and Discussion

Plotting the values of the forces in the z-direction gives us the graph as seen in Figure 4. As the testing begins, the relative z-loads increase in amplitude as expected. Over each 10 degree jump in peak-peak amplitude, the forces generated in the z-direction are shown to proportionally increase. Figure 5 shows the sum of forces in the z-direction measured by individual load cells over a test period of 5 seconds. This is compared with a theoretical sinusoidal model

assumed from a similar flat plate with a matched phase and frequency.

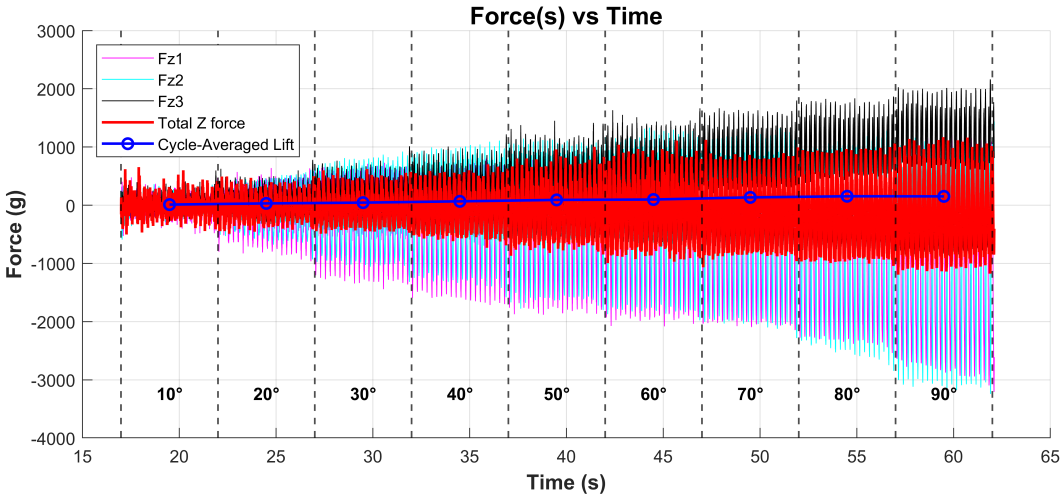

Fig. 4 All Forces in the Z-direction

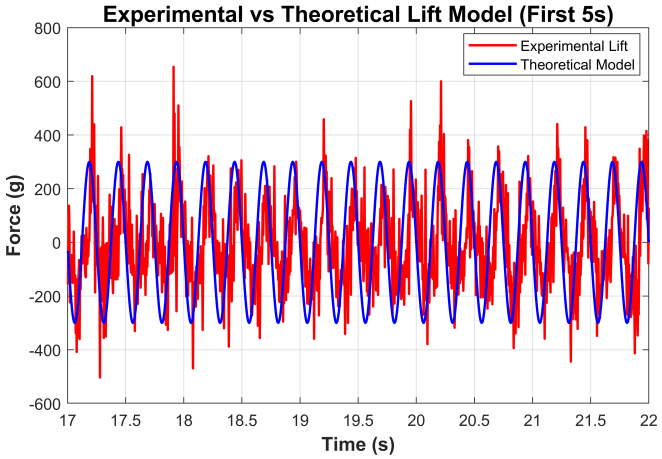

Fig. 5 Periodic variations of combined z-loads over a 5 second test period.

The model is similar, although there is much noise in the system and there seems to be vibrations within the frequency itself noting additional disturbances from a lack of stiffness in the structure. Potential disturbances due to EMF of the high current high power motor are also a concern that may be worth noting to characterize in the future.

The primary mode of positive (downward stroke) and negative (upward) lift is attributed to the leading edge vortex formation being situated close to the surface. The presence of a strong 3D spiraling attached vortex provides unsteady lift over the flat plates. Theoretically, based on the flat plate at zero angle of attack, the expected cycle averaged lift would be zero. However, a general positive lift trend was observed with the increasing flapping amplitude. The two graphs shown in Figure 6, show the Lift and Thrust variations over the various peak-peak amplitudes. Since the frequency is fixed at 4 Hz and the data was sampled over a period of 5 seconds, each cycle averaged value is derived from 20 cycles of flapping. This positive cycle average lift is possibly due to the wing stiffners being only on the undersurface creating an asymmetric camber during the downward and upward stroke, a fortunate coincidence!

The leading edge suction pressure intensifies with the increasing amplitude which can be modeled as the volume of air that is displace by the wing. This z-velocity component is the driving factor in the increasing lift forces. There is some indication of the lift to drop off beyond its maximum value observed at a peak-peak amplitude of 80°.

The values we see for cycle-averaged thrust are fitting as well. K1 has only one hinge point at the root for each wing, where the reacting forces can be modeled as a net effect of bending and torsional modes. The presence of the stiffners on

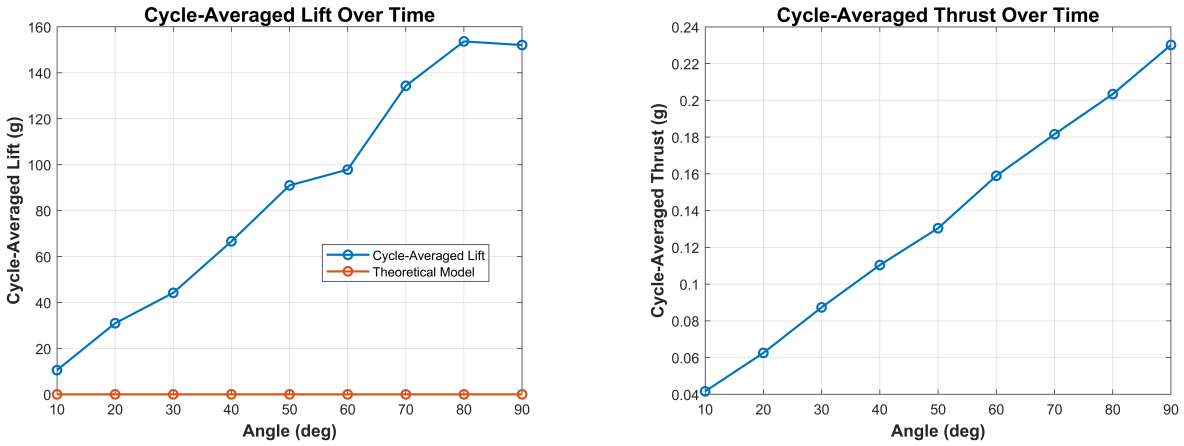

(a) Cycle Averaged Lift Values **(b) Cycle Averaged Thrust Values**

Fig. 6 Comparison of Cycle Averaged Lift and Thrust Values

the wing being only on the underside is possibly adding twist along the span, sufficient to create resultant force (vector sum of lift and thrust) vectoring, resulting in thrust force. This thrust is directly proportional to both amplitude and frequency, any increase/decrease in either amplitude or frequency will result in a respectively proportional changes in thrust.

A. Applicable Insight

When optimizing the cruise flight conditions of a flapping-wing aerial vehicle, a common equation to optimize the stroke amplitude is typically determined using the Strouhal number equation:

$$St = \frac{fL_d}{U} = \frac{2fh_a}{U}$$

where St is the Strouhal number, f is the flapping frequency, U is the forward velocity, and h_a represents the half-stroke amplitude—the vertical distance from the wingtip's horizontal position to its highest point during the upstroke[12]. Given a set forward speed from wing design, an ideal Strouhal number of 0.3, and a frequency characterized by the mass of the FWAV, most FWAV's will generally fall into a peak amplitude range of 60±20 degrees to operate optimally.

This makes the current flapping mechanism design capable of optimizing towards any size or speed of FWAV given its large range of operational amplitudes and frequencies. Although the testing shown only showcased a maximum peak-peak amplitude of 90 degrees, future testing will include amplitudes upwards of 180 degrees ensuring full coverage of all flight angle capabilities, with wind-on cases.

VI. Conclusion

This study demonstrated the aerodynamic force characteristics of a novel bio-mimetic variable amplitude flapping mechanism successfully achieving flapping amplitudes between 10 and 90 degrees at a fixed frequency of 4 Hz. The mechanism produced sufficient lift and thrust to validate its feasibility for FWAVs. The results indicate increasing amplitude correlation with greater lift generation, aligning with theoretical predictions of the unsteady aerodynamics in flapping flight.

The cycle-averaged lift data revealed a coincidental positive trend with increasing amplitude suggesting favorable asymmetric camber effects. The cycle-averaged thrust data further confirmed the proportionality of flapping amplitude to tangential velocity and thrust respectively. The findings provide valuable initial validation that the flapping mechanism implemented on K1 and the load cell test setup provide a good basis for further testing of various wings, amplitudes, and frequencies moving forward.

Further work is needed to refine and validate these results. A full-scale CFD analysis can be conducted to compare experimental data with prior theoretical work and further characterize the aerodynamic performance of the system.

Additional tests can be performed to evaluate the full 180° peak-to-peak amplitude range and its effect on lift and thrust, including for oncoming wind on cases. Another important consideration is motor EMF, which was not accounted for in this study but could be affecting sensor readings and adding noise to the measured forces at high loads.

Past static bench testing, K1 flight trials will be held soon, which is further critical to assessing how the system performs in real-world conditions.

VII. Acknowledgements

The authors thank the Graduate Education office for their financial support to build the system. The authors thank the invaluable facilities of Cal Poly's Machine Shops.

References

[1] Ajanic, E., Feroskhan, M., Mintchev, S., Noca, F., and Floreano, D., "Bioinspired wing and tail morphing extends drone flight capabilities," *Science Robotics*, Vol. 5, No. 47, 2020, p. eabc2897. https://doi.org/10.1126/scirobotics.abc2897, URL https://www.science.org/doi/10.1126/scirobotics.abc2897.

[2] Bishay, P. L., Brody, M., Podell, D., Corte Garcia, F., Munoz, E., Minassian, E., and Bradley, K., "3D-Printed Bio-Inspired Mechanisms for Bird-like Morphing Drones," *Applied Sciences*, Vol. 13, No. 21, 2023, p. 11814. https://doi.org/10.3390/app132111814, URL https://www.mdpi.com/2076-3417/13/21/11814.

[3] Chang, E., Matloff, L. Y., Stowers, A. K., and Lentink, D., "Soft biohybrid morphing wings with feathers underactuated by wrist and finger motion," *Science Robotics*, Vol. 5, No. 38, 2020, p. eaay1246. https://doi.org/10.1126/scirobotics.aay1246, URL https://www.science.org/doi/10.1126/scirobotics.aay1246.

[4] Zhang, J., Zhao, N., and Qu, F., "Bio-inspired flapping wing robots with foldable or deformable wings: a review," *Bioinspiration & Biomimetics*, Vol. 18, No. 1, 2022, p. 011002. https://doi.org/10.1088/1748-3190/ac9ef5, URL https://dx.doi.org/10.1088/1748-3190/ac9ef5, publisher: IOP Publishing.

[5] Pennycuick, C. J., "Power Requirements for Horizontal Flight in the Pigeon *Columba Livia*," *Journal of Experimental Biology*, Vol. 49, No. 3, 1968, pp. 527–555. https://doi.org/10.1242/jeb.49.3.527, URL https://journals.biologists.com/jeb/article/49/3/527/21322/Power-Requirements-for-Horizontal-Flight-in-the.

[6] Tobalske, B. W., and Dial, K. P., "Flight Kinematics of Black-Billed Magpies and Pigeons Over a Wide Range of Speeds," *Journal of Experimental Biology*, Vol. 199, No. 2, 1996, pp. 263–280. https://doi.org/10.1242/jeb.199.2.263, URL https://journals.biologists.com/jeb/article/199/2/263/7465/Flight-Kinematics-of-Black-Billed-Magpies-and.

[7] Warrick, D. R., and Dial, K. P., "Kinematic, Aerodynamic and Anatomical Mechanisms in the Slow, Maneuvering Flight of Pigeons," *Journal of Experimental Biology*, Vol. 201, No. 5, 1998, pp. 655–672. https://doi.org/10.1242/jeb.201.5.655, URL https://doi.org/10.1242/jeb.201.5.655.

[8] Huang, H., He, W., Wang, J., Zhang, L., and Fu, Q., "An All Servo-Driven Bird-Like Flapping-Wing Aerial Robot Capable of Autonomous Flight," *IEEE/ASME Transactions on Mechatronics*, Vol. 27, No. 6, 2022, pp. 5484–5494. https://doi.org/10.1109/TMECH.2022.3182418, URL https://ieeexplore.ieee.org/document/9805830/?arnumber=9805830, conference Name: IEEE/ASME Transactions on Mechatronics.

[9] Gerdes, J., Holness, A., Perez-Rosado, A., Roberts, L., Greisinger, A., Barnett, E., Kempny, J., Lingam, D., Yeh, C.-H., Bruck, H. A., and Gupta, S. K., "Robo Raven: A Flapping-Wing Air Vehicle with Highly Compliant and Independently Controlled Wings," *Soft Robotics*, Vol. 1, No. 4, 2014, pp. 275–288. https://doi.org/10.1089/soro.2014.0019, URL https://www.liebertpub.com/doi/10.1089/soro.2014.0019.

[10] Chen, A., Song, B., Wang, Z., Xue, D., and Liu, K., "A Novel Actuation Strategy for an Agile Bioinspired FWAV Performing a Morphing-Coupled Wingbeat Pattern," *IEEE Transactions on Robotics*, Vol. 39, No. 1, 2023, pp. 452–469. https://doi.org/10.1109/TRO.2022.3189812, URL https://ieeexplore.ieee.org/document/9849140/, conference Name: IEEE Transactions on Robotics.

[11] Kim, P., and Hiremath, N., "Design and Fabrication of a Customizable Multi-Axis Load Cell with Commercial Off-The-Shelf Components," *2024 Regional Student Conferences*, American Institute of Aeronautics and Astronautics, Multiple Locations, 2024. https://doi.org/10.2514/6.2024-81658, URL https://arc.aiaa.org/doi/10.2514/6.2024-81658.

[12] Hassanalian, M., Abdelkefi, A., Wei, M., and Ziaei-Rad, S., "A novel methodology for wing sizing of bio-inspired flapping wing micro air vehicles: theory and prototype," *Acta Mechanica*, Vol. 228, No. 3, 2017, pp. 1097–1113. https://doi.org/10.1007/s00707-016-1757-4, URL https://doi.org/10.1007/s00707-016-1757-4.